promoting access to White Rose research papers

Universities of Leeds, Sheffield and York
http://eprints.whiterose.ac.uk/

This is an author produced version of a paper published in **Composites Part B: Engineering**.

White Rose Research Online URL for this paper:
http://eprints.whiterose.ac.uk/42823

Published paper

Pesic, N., Pilakoutas, K. (2003) *Concrete beams with externally bonded flexural FRP-reinforcement: analytical investigation of debonding failure*, Composites Part B: Engineering, 34 (4), pp. 327-338
http://dx.doi.org/10.1016/S1359-8368(02)00139-7

White Rose Research Online
eprints@whiterose.ac.uk

Concrete Beams with Externally Bonded Flexural FRP-Reinforcement: Analytical Investigation of Debonding Failure

Ninoslav Pe{i}*, Kypros Pilakoutas

The University of Sheffield, Department of Civil and Structural Engineering
Mappin Street, Sir Frederick Mappin Building, Sheffield, S1 3JD, UK
(*corr.author's e-mail address*: n.pesic@sheffield.ac.uk)

Elsevier Composites Part B: Engineering

Abstract

This paper studies the problem of early concrete cover delamination and plate-end failure of reinforced concrete beams strengthened with externally bonded FRP-reinforcement. The accuracy of analytical models and finite element (FE) methods for predicting this type of failure is assessed against published experimental data. Two design approaches based on the maximum concrete tensile strength and the shear capacity of concrete beams were examined first and it was found that linear elastic analysis can not accurately predict the brittle plate-end. It was also found that the extent of strengthening that can be achieved is limited by the shear capacity of concrete beams. The FE analysis is used to examine the effects of internal tensile reinforcement on the magnitude principal tensile stresses in the critical region. The non-linear behaviour of FRP-strengthened beams is also examined in the FE analysis using the smeared crack model for concrete which is shown to adequately display the inelastic deformation of the beam. Finally, the mixed mode of failure due to the combined shear and concrete cover delamination is addressed through modelling plate-end and shear crack discontinuities using the discrete crack approach.

Keywords: Concrete [A], FRP-reinforcement [A], Delamination [B], Finite element analysis [C].

Introduction

For more than a decade, FRP composites are being used in the construction industry in the form of laminates and pultruded plates for strengthening of existing concrete bridges (Fig.1-a) and other structures [1]. With their excellent properties such as high tensile strength, long-term durability, corrosion/fire resistance and low weight, FRPs have almost completely replaced steel plates as externally epoxy-bonded reinforcement for concrete. As flexural reinforcement, FRP-plates significantly increase the stiffness and load capacity of concrete beams, but decrease their ductility and often result in brittle failure modes which are not desirable in structural design. Thus, the most frequent and studied type of failure is the delamination of FRP-plate and the adjacent concrete cover (Fig.1-b) due to the normal and shear stress concentration at the end of the bonded plate.

The theory of stress analysis for metalic/plastic structural elements with cemented joints subjected to both axial and bending deformation was first established by Goland and Reissner [2]. Volkersen [3] provided governing equations for normal and shear stress distributions in double-lap cemented joints which were later improved in 1970's as reviewed in [4]. Roberts [5] further developed governing equations valid for different adhesive joint configurations subjected to bending and axial forces and indicated the role of practical details such as spew fillets of adhesive on reduction of stress concentration. Most of these early studies preceeded the application of bonded steel-plates for concrete strengthenening and the development of Roberts and Haji-Kazemi's solution based on the partial interaction theory [6] which relaxed bondary condition for zero shear stress on the free edge of adhesive. With the introduction of FRP-materials to plate-bonding of concrete elements, the work of Roberts [6] was followed by a number of analytical solutions based on linear elastic method [7-10]. These solutions were found to produce very similar stress magnitudes in the debonding zone [10]. Still, their ability to predict debonding failures has not yet been verified against experimental data from published works although several concrete design guidelines are already being extended to comprise the FRP-plate strengthening technique [11-12].

This paper aims to review and assess the accuracy of available methods to predict the load level at which FRP-plated concrete beams fail due to plate-end debonding. Apart from the common maximum tensile stress criterion, the application of the so-called 'shear capacity' criterion is investigated and comparisons are made with experimental data. The experimental data were collected from published experimental research work on FRP-plated beams without any additional mechanical anchorages.

Recently, Teng at al. [13] presented stress contour plots of the FRP-anchorage zone based on the linear finite element (FE) analysis showing a very complex stress pattern in which the adhesive-FRP interface is subjected to compression while, as expected, the tension develops on the adhesive-concrete interface.

An aspect which has not been studied extensively in FE analysis is the effect of the non-linear material characteristics and the applicability of non-linear (NL) FE analysis is examined and demonstrated for several experimentally tested beams. Apart from the material non-linear properties, the NL FE analysis is also used to analyse models of FRP-strengthened beams with various configurations of crack discontinuities. In all experiments, cracks were observed within the shear before the final plate-end debonding, leading to a combined shear and plate-end debonding failure.

Analytical Models

When a simply supported reinforced concrete (RC) beam of arbitrary section and with externally bonded FRP-plate is subjected to flexural loading, high tensile and shear stresses develop in the concrete and adhesive layer at the plate end. This bi-axial state of tension comprises the tensile stress components due to bending, σ_x, the shear stresses, τ_a, and normal peeling stresses, σ_n, due to the transfer of tensile force from the bonded FRP-plate through the adhesive layer to the concrete. As a result, to guard against the brittle plate-end failure, a maximum tensile stress criterion for concrete $\sigma_1 < f_{ct,m}$ has been incorporated in design recommendations [11, 14]. The principal tensile stress in concrete at the critical section is defined by:

$$\sigma_1 = \frac{\sigma_x + \sigma_{n,\max}}{2} + \sqrt{\left(\frac{\sigma_x - \sigma_{n,\max}}{2}\right)^2 + \tau_{a,\max}^2} \qquad (1)$$

while the mean concrete tensile strength, $f_{ct,m}$, for a known concrete compressive strength f_{ck}, can be taken as $f_{ct,m} \approx 0.30 f_{ck}^{2/3}$ (MPa).

The differences between various analytical models arise from the way in which the maximum stress components $\sigma_{n,max.}$ and $\tau_{a,max.}$ at the plate-end section are obtained. For example, the *fib* design guidelines [11] recommends the use of the approximate Roberts' model [15] for the calculation of $\sigma_{n,max.}$ and $\tau_{a,max.}$ but, contrary to [14], it doesn't take into account the influence of bending stress σ_x. However, for the validation of the maximum

tensile stress criterion, a more recent solution for calculation of $\sigma_{n,max.}$ and $\tau_{a,max.}$ given by Smith and Teng [10] is adopted in this study. When the FRP-plated beam is subjected to two concentrated loads (Fig.2), the governing differential equations for shear and normal interface stresses, $\tau_a(x)$ and $\sigma_n(x)$, giving the maximum values of $\tau_{a,max}$ and $\sigma_{n,max}$ for $x=0$ (at the end of bonded FRP-plate), in the authors' original notation [10], are:

$$\frac{d^2\tau_a(x)}{dx^2} - \frac{G_a b_2}{t_a}\left[\frac{1}{E_1A_1} + \frac{1}{E_2A_2} + \frac{(y_1+y_2)(y_1+y_2+t_a)}{E_1I_1}\right]\tau_a(x) = -\frac{G_a}{t_a}\left(\frac{y_1+y_2}{E_1I_1+E_2I_2}\right)P \quad (2)$$

$$\frac{d^4\sigma_n(x)}{dx^4} + \frac{E_a b_2}{t_a}\left[\frac{1}{E_1I_1} + \frac{1}{E_2I_2}\right]\sigma_n(x) = \frac{E_a b_2}{t_a}\left[\frac{y_2}{E_2I_2} - \frac{y_1}{E_1I_1}\right]\frac{d\tau_a(x)}{dx} \quad (3)$$

where E_1, A_1, I_1 are the Young's modulus, cross-section area and second moment of area for concrete element; E_2, A_2, I_2, b_2 are the Young's modulus, cross-section area, second moment of area and the width of bonded plate; P is the applied shear force; E_a, G_a and t_a are the elastic modulus, shear modulus and the thickness of the adhesive layer, respectively, while y_1 and y_2 are the distance from the centroid of plated composite section to the centroid of concrete and to the centroid of plate section alone.

Verification of the Maximum Tensile Stress Criterion

A large number of experimental results for FRP-strengthened concrete beams which have failed due to the plate-end debonding is reported in the literature. As not all of the published works provide all the information for back analysis, for the purpose of this investigation, 77 beams providing sufficient information were selected for the analysis. By using these data and the above analytical approach, the principal tensile stress was calculated for the reported beam failure load using Eq.(1) and the results are given in column σ_1 of Table 1. When the bending stress σ_x at the plate-end point exceeded the concrete tensile strength, the σ_x stress component was omitted from Eq.(1) and the new results are then provided in column σ_{1^*}. The total failure load P_{fail} and the corresponding maximum bending moment M_{max}, FRP-plate material, span of the beam (L) and concrete characteristic strengths (f_{ck}, f_{ctm}) are also shown for each beam. For the complete record, the reader is referred to the original works.

The analytical predictions for σ_1 are often considerably different from the estimated concrete tensile strength, indicating that some assumptions in the linear elastic analysis may not be valid for concrete beams. Beams A950, A1100 and A1150 tested by Nguyen [28] show almost no sign of reduction in load capacity when shorter plates are used despite the fact that the principal stress computed for the beam with 950 mm plate is almost twice that of the beam with 1150 mm long plate. However, the series of beams B3, B4, B5 and B6 tested by Rahimi and Hutchinson [29] and beams DF.2, DF.3 and DF.4 tested by Ahmed and Van Gemert [25] exhibited an increase in load capacity with an increase in plate thickness, which is the opposite from what is expected from the analysis for plate-end debonding failures. For only two series of tested beams did the elastic analysis produce values of σ_1 and σ_{1^*} which are reasonably close to the concrete tensile strength. In all other cases, the calculated principal stresses σ_1 and σ_{1^*} largely either over- or underestimate the actual stress at critical plate-end section and it appears that their magnitudes are strongly affected by the non-linear behaviour of concrete and the presence of shear and flexural cracks.

Other uncertainties reflected in the large scatter of obtained results can be related to the determination of concrete shear and tensile strength and to other parameters such as the effective flexural reinforcement ratio (considered later in the analysis). In the following section, a different approach based on the flexural and shear capacity of FRP-plated beams is examined.

Shear and Flexural Capacity of FRP-strengthened Beams

Shear Capacity

The characteristic shear resistance of the FRP-strengthened concrete beams, listed in Table 1 under column V_{ck}, was evaluated in accordance with *fib*/Eurocode 2 [11] but, in principle, any national design code can be used instead. By using a numerical procedure for flexural analysis of FRP-strengthened beams [31], the following values were also

calculated and shown in Table 1: the yielding bending moment of originally non-strengthened beam M_y, the yielding bending moment of FRP-strengthened beam $M_{y,f}$, and the ultimate bending moment for plated beam, $M_{u,f}$.

With respect to the shear capacity of strengthened beams, a very interesting observation can be made on the results for the eight specimen series tested by Ross at al. [26]. All these beams had the FRP-plates extended over the supports and, although no geometric conditions for stress concentration existed within the shear span, the beams still failed in brittle manner with delamination of the plate at the load level of the calculated shear resistance, V_{ck}. It appears that, regardless of the plate termination point (within or outside the span), the presence of high-strength FRP-materials on the tension side of concrete beams leads to an increase in tensile and shear stresses in the concrete cover within the shear span. As this concrete layer is not confined by internal steel shear reinforcement, the tensile force from the bonded FRP-reinforcement can not be transferred to the internal concrete core and, as a result, the beams fail when the shear capacity of the equivalent unreinforced concrete element is exceeded by the applied loading.

The calculated data for all beams are graphically presented in a form of (V_{shear}/V_{ck}) versus ($M_{max}/M_{y,f}$) diagram shown in Figure 3. From this graph, it is very difficult to establish any clear relation between the achieved shear and flexural capacities of plated beams, but there is a strong indication that the shear resistance of the FRP-strengthened beams is limited by the shear resistance of the equivalent concrete beams without shear reinforcement. For preliminary design of normally plated beams (plate ends before the supports), the applied shear force can be limited by the following simple shear capacity criterion which is essentially very similar to the one proposed by Smith and Teng [32]:

$$V_{pd} \leq 0.8V_{ck} \tag{4}$$

For beams with plates extended under the supports or having additional anchorages the applied shear force V_{pd} can be taken to be equal to V_{ck}.

Another way of assessing the effectiveness of FRP-strengthening is to examine the ratios of moment capacities of strengthened beams to the yielding moment of the originally non-strengthened beams, M_y, as shown in Fig.4. This figure shows that for those beams which failed due to plate-end debonding, the typical ratio of $M_{y,f}/M_y$ varies from 115 to 150%. However, on several occasions the failure took place before the applied load reached the yielding capacity of the strengthened or, even worse, the previously unstrengthened beams. Apparently, the effectiveness of strengthening is not independent from the flexural capacity of previously unstrengthened beams.

Figure 5 shows a reduction trend in the utilisation of the full flexural capacity of strengthened beams ($M_{max}/M_{u,f}$) with an increase in the level of FRP-strengthening expressed as ρ_{eff}/ρ_s, where the effective reinforcement ratio is taken as $\rho_{eff} = \rho_s + \rho_f E_f / E_s$ and E_f and E_s are the moduli of elasticity for FRP and steel reinforcement, respectively. This means that the use of disproportionate amounts of FRP reinforcement does not lead to an efficient solution.

The above findings indicate that the capacity design can not be used for safe and economic design. Many parameters such as the amount of internal (existing) and external (new) reinforcement are not taken into detailed consideration although, as demonstrated here, they do have an influence on the load level corresponding to brittle delamination failures. Hence, a more thorough investigation of the problem is required and for this purpose the results from linear elastic and non-linear finite element analysis are examined next.

Finite Element Analysis

Linear elastic analysis

The finite element analysis of the experimentally tested FRP-plated concrete beams was conducted using the ABAQUS commercial package [33]. As none of the existing analytical models takes into consideration the presence of internal steel reinforcement, its influence is investigated first assuming, for simplicity, that concrete behaves ideally elastic in tension.

Properties of adhesives and FRP laminates used in the analysis are as given in the referenced works [16-30]. The Young's modulus of the adhesive E_a can range from 2 to 12 *GPa* and its Poisson's coefficient ν_a is approximately 0.35-0.37. The FRP-reinforcement is modelled as ideally elastic orthotropic material. The characteristic tensile strength f_{fk} and mean Young's modulus E_f define the tensile fracture strain in the direction parallel to fibres as $\varepsilon_{fk}=f_{fk}/E_f$. The minor elastic modulus in the transverse direction, $E_{f\perp}$, has a typical value of 5-20% of E_f depending on the FRP material and the fibre to matrix volume fraction.

Finite element models of FRP-plated beams, with refined mesh in the plate-end region, in general indicate a variation in both normal and shear stresses across the thickness of the adhesive layer. This can be seen from Figure 6-a showing the contour plot of principal tensile stresses at the plate anchorage zone for beam $B_u2.3$ [23].

The FE analysis also shows that, for the same beam, the principal stresses on the concrete-adhesive interface in the plate anchorage zone are significantly reduced by the presence of longitudinal steel reinforcement (Fig.6-b). The spew fillets of adhesive can additionally improve the local stress field reducing the principal tensile stresses for about 10-15% (Fig.6-c). Further graphical comparison between the analytical and FE solutions for different reinforcement ratios is given in Figure 7.

The peak principal stresses in concrete at the plate-end were computed for the reported failure loads and are listed in Table 1 as $\sigma_{1,fe}$ and $\sigma_{1,fe,r}$, where the latter symbol denotes the values obtained when the steel reinforcement is modelled with 'rebar' elements embedded in concrete. These results show an overall trend of stress reduction with an increase in the amount of tensile steel reinforcement as seen from Fig.8.

However, even the stress values obtained from linear FE analysis, when internal reinforcement was taken into account, are unable to accurately predict the failure load for the majority of the tested beams. One of the main reasons for this inaccuracy may be a high variability in the concrete tensile strength, as well as the inability of elastic analysis to properly take into account the actual non-linear behaviour of concrete.

Constitutive Material Models for Non-linear FE analysis

Apart from the non-linear material characteristics, the response of the strengthened beams may be significantly affected by the presence of material discontinuities in the form of crack openings. The investigation of these effects is done through non-linear FE analysis, using both the discrete and smeared-crack model, with tension softening for concrete as shown in Figure 9 [34]. In the non-linear FE analysis, the epoxy adhesive (after curing and hardening) and internal steel reinforcement are considered to be ideal isotropic elasto-plastic materials.

Non-linear FE analysis

Although reported as beams which failed exclusively in brittle manner with plate-end debonding, many of these beams developed major shear cracks from which the interface cracks further propagated towards the ends of the bonded FRP-plates until failure. The non-linear FE analysis is used here in an attempt to predict the complicated stress/strain states for such beams. To examine the possible effects of the crack opening on the stress distribution in the anchorage zone, another focused mesh geometry, shown in Fig.10-a, is used in the FE models to study the redistribution of stresses and strains along the concrete-adhesive interface after the formation of the shear and the plate-end

cracks. The figure shows that after the formation of the plate-end crack, the stress concentration follows the crack which, as reported in all experiments, with a small load increment becomes unstable leading to the brittle concrete cover delamination failure.

In the case illustrated in Fig.10-b, showing the total strain when only the shear crack is present, a considerable increase in principal strains can be detected in the adhesive layer near the shear crack. This indicates a possible crack propagation along the concrete-adhesive interface starting from the shear crack opening towards the plate-end. This can lead to a type of failure reported in the past which typically results in the separation of the FRP-plate and adjacent thin concrete layer from the beam [20, 22, 23, 29].

The approach with discrete crack modelling can, however, only be applied in the analysis if the location of shear cracks is known in advance (almost never the case in practice), but the same phenomenon can be studied using the smeared crack approach. Due to the nature of the concrete tension softening model, non-linear FE analysis based on the smeared crack model can not give the stresses in the critical zone which are directly comparable to those obtained from elastic analysis, but it can produce a better picture of the strain distribution throughout the strengthened beam.

Figures 11-a and 11-b show contour plots of the principal inelastic strains which reasonably accurately display the damage of beam A7 which failed due to the combined effects of shear and plate-end debonding [29]. It can be observed that the magnitudes of tensile strains in the mid-span are always higher than the magnitudes within the shear span. However, the high tensile strains in the mid-span correspond to stabilised flexural cracks while those within the shear span are potentially more dangerous. As the shear crack propagates down to the bonded FRP-plate, the damage zone is also extending to the unreinforced concrete layer between the internal steel and external FRP reinforcement creating conditions for brittle failure due to the combined shear and debonding. It can be

said that the non-linear FE analysis has identified, at least quantitatively, the role of the shear crack formation which has, in many reported cases, influenced the mode of failure and the ultimate load capacity of FRP-strengthened concrete beams.

Conclusions

This study investigated the applicability of different analytical approaches for predicting the capacity of FRP-strengthened concrete beams and made comparisons with results of 77 experimentally tested beams which failed due to the plate-end debonding. The main conclusions are summarised as follows:

- The examined analytical and finite element linear elastic solutions for the plate end stress concentration do not appear to be very accurate in predicting the plate end concrete cover failures. Apart from the variability related to the concrete tensile strength, the presence of tensile steel reinforcement, the non-uniform stress distribution through the adhesive layer, the overall non-linear response of strengthened beams and flexural and shear crack openings are thought to be the main reasons which have led to a large scatter of obtained results.
- Since the stress levels at which debonding failure modes occur can not be measured directly and in view of other uncertainties arising from the experimental data, appropriate partial safety factors applying to the plate end concrete cover failure will still be required even after the improvements are made over the analytical models based on linear elastic analysis.
- In preliminary design of FRP-plated beams, the detailed analysis of stress concentration can be omitted provided that the applied shear force does not exceed $0.80V_{ck}$ (or just V_{ck} if the FRP-plates are extended over the supports).

- The finite element analysis shows that, by taking into account the internal steel reinforcement, the calculated values of peak normal stresses in concrete at the plate-termination point are, in average, reduced by 20-40%.
- The FE analysis indicates that spew fillets of adhesive can provide 10-15% further reduction of tensile stresses in concrete at the plate-end zone.
- The formation of shear cracks in concrete was simulated in 2-D non-linear FE analysis and it was verified that the excessive propagation of these cracks down to the level of bonded FRP-reinforcement can affect the final failure mode. At the opening of shear crack, a stress concentration in concrete and the adhesive layer can lead to further crack propagation along the concrete-adhesive interface towards the plate-end.

In general, the application of the finite element method raises the question as to how the influence of shear cracks, whose exact locations is difficult to predict, can be properly addressed in the analysis and it is not immediately obvious how the associated effects of dowel action and aggregate interlock can be taken into account at the design stage. The non-linear FE analysis was demonstrated to have predicted inelastic deformation in the strengthened beam identifying the brittle failure mode. It was also used to determine the stress-strain distribution in the presence of shear crack discontinuities which also lead to delamination failures.

Acknowledgements

The authors are grateful for the financial support received from the British Universities ORS award scheme and E.U. Commission who funded the 'TMR' ConFibreCrete research network).

References:

[1] Meier U., "Strengthening of structures using carbon fibre/epoxy composites", ELSEVIER Construction and Building Materials, 1995; 9(6):341-351.

[2] Goland M. and Reissner E., "The stresses in cemented joints", ASME Journal of Applied Mechanics, 1944; 11(1):A17-A27.

[3] Volkersen O., "Recherches sur la theorie des assemblages colles", Construction Metallique, 1965; 4(1):3-13.

[4] Adams R.D. and Wake W.C., "Structural Adhesive Joints in Engineerins", (ELSEVIER Applied Science) London/New York, 1984.

[5] Roberts T.M., "Shear and normal stresses in adhesive joints", ASCE Journal of Engineering Mechanics, 1989; 115(11):2460-2479.

[6] Roberts T.M. and Haji-Kazemi H., "Theoretical study of the behaviour of reinforced concrete beams strengthened by externally bonded steel plates", in: Procs.Institution of Civil Engineers (Part 2), 1989; 87(3):39-55.

[7] Taljsten B., "Strengthening of beams by plate bonding", ASCE Journal of Materials in Civil Engineering, 1997; 9(4):206-212.

[8] Malek A.M., Saadatmanesh H. and Ehsani M.R., "Prediction of failure load of R/C beams strengthened with FRP plate due to stress concentration at the plate end", ACI Structural Journal, 1998; 95(1):142-152.

[9] Lau K.T., Dutta P.K., Zhou, L.M. and Hiu D., "Mechanics of bonds in an FRP bonded concrete beam", ELSEVIER Composites Part B: Engineering, 2001; 32(6):491-502.

[10] Smith S.T. and Teng J.G., "Interfacial stresses in plated beams", ELSEVIER Engineering Structures, 2001; 23(3):857-871.

[11] "Externally bonded FRP reinforcement for RC structures", Bulletin No. 14, *fib* CEB-FIP, 2001.

[12] "Strengthening of Reinforced Concrete Structures with Externally-Bonded Fibre Reinforced Polymers", Design Manual No.4, ISIS CANADA, September 2001.

[13] Teng J.G., Zhang J.W. and Smith S.T., "Interfacial stresses in reinforced concrete beams bonded with a soffit plate: a finite element study", ELSEVIER Construction and Building Materials, 2002; 16(1):1-14.

[14] Saadatmanesh H. and Malek A.M., "Design guidelines for flexural strengthening of RC beams with FRP plates", ASCE Journal of Composites for Construction, 1998; 2(4):158-164.

[15] Roberts T.M., "Approximate analysis of shear and normal stress concentration in the adhesive layer of plated RC beams", The Structural Engineer, 1989; 67(12):229-233.

[16] Saadatmanesh H. and Ehsani M.R., "RC beams strengthened with GFRP plates I: Experimental study", ASCE Journal of Structural Engineering, 1991; 117(11):3417-3433.

[17] Ritchie P.A., Thomas D.A., Lu L.W. and Connelly G.M., "External reinforcement of concrete beams using fiber reinforced plastic", ACI Structural Journal, 1991; 88(4):490-500.

[18] Triantafillou T.C. and Plevris N., "Strengthening of R.C. beams with epoxy-bonded fibre-composite materials", RILEM Materials and Structures, 1992; 25(148):201-211.

[19] Sharif A, Al-Suleimani G.J., Basanbul I.A., Baluch M.H. and Ghaleb B.N., "Strengthening of initially loaded reinforced concrete beams using FRP plates", ACI Structural Journal, 1994; 91(2):160-168.

[20] Quantrill R.J., Holloway L.C. and Thorne A.M., "Predictions of the maximum plate and stresses of FRP strengthened beams: Part II", Magazine of Concrete Research, 1996; 48(177):331-342.

[21] Arduini M., Di Tommaso A. and Nanni A., "Brittle failure in FRP plate and sheet bonded beams", ACI Structural Journal, 1997; 94(4):363-370.

[22] He J.H., "Behaviour of Reinforced Concrete Beams Strengthened with Epoxy Bonded CFRP Plates", PhD Thesis, The University of Sheffield, 1998.

[23] Garden H.N., Quantrill R.J., Hollaway L.C., Thorne A.M. and Parke G.A.R., "An experimetnal study of the anchorage length of carbon fibre composite plates used to strengthen reinforced concrete beams", ELSEVIER Construction and Building Materials, 1998; 12(4):203-219.

[24] Spadea G., Bencardino F. and Swamy R.N., "Structural behavior of composite RC beams with externally bonded CFRP", ASCE Journal of Composites for Construction, 1998; 2(3):132-137.

[25] Ahmed O. and Van Gemert D., "Effect of longitudinal carbon fiber reinforced plastic laminates on shear capacity of reinforced concrete beams", In: Proceedings of Fiber Reinforced Polymer Reinforcement for RC, Baltimor, USA, 1999, p.933-943.

[26] Ross A.C., Jerome D.M, Tedesco J.W. and Hughes M.L., "Strengthening of reinforced concrete beams with externally bonded composite laminates", ACI Structural Journal, 1999; 96(2):212-220.

[27] Ramana V.P.V, Kant T., Morton S.E., Dutta P.K., Mukherjee A. and Desai Y.M., "Behavior of CFRP strengthened reinforced concrete beams with varying degrees of strengthening", ELSEVIER Composites Part B: Engineering, 2000; 31(6-7):461-470.

[28] Nguyen D.M., Chan T.K. and Cheong H.K., "Brittle failure and bond development length of CFRP-concrete beams", ASCE Journal of Composites for Construction, 2001; 5(1):12-17.

[29] Rahimi H. and Hutchinson A., "Concrete beams strengthened with externally bonded FRP plates", ASCE Journal of Composites for Construction, 2001; 5(1):44-56.

[30] Fanning P.J. and Kelly O., "Ultimate response of RC beams strengthened with CFRP plates", ASCE Journal of Composites for Construction, 2001; 5(2):122-127.

[31] Pe{i} N., "Analysis and Design of R.C. Beams with Externally Bonded FRP-Reinforcement", PhD Thesis, The University of Sheffield, (to be published early in 2003), or [31] "Numerical analysis and design of reinforced concrete beams with externally bonded FRP reinforcement", paper submitted for possible publication in (RILEM) Journal of Materials and Structures (2003).

[32] Smith S.T. and Teng J.G., "Strength models for plate end debonding in FRP-strengthened RC beams", In: Fibre-Reinforced Plastics for Reinforced Concrete Structures - FRPRC 5, Cambridge, UK, 2001, p.419-428.

[33] ABAQUS, FEA Software and User's Manual v5.8, Hibbitt, Karlsson & Sorensen Inc., http://www.abaqus.com, 1998.

[34] Kwak H.G. and Kim S.P., "Non-linear analysis of RC beams based on moment-curvature relation", Elsevier Computers & Structures, 2002; 80(7-8):615-628.

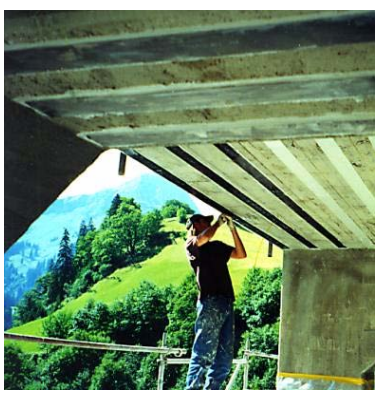

a)

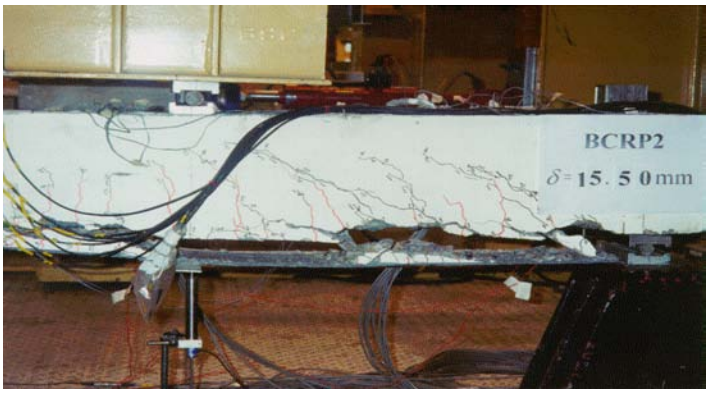

b)

Figure 1: Application of externally bonded FRP reinforcement: a) bridge strengthening (courtesy of S&P Reinforcement GmbH, Switzerland); b) typical delamination failure of experimentally tested beam [22].

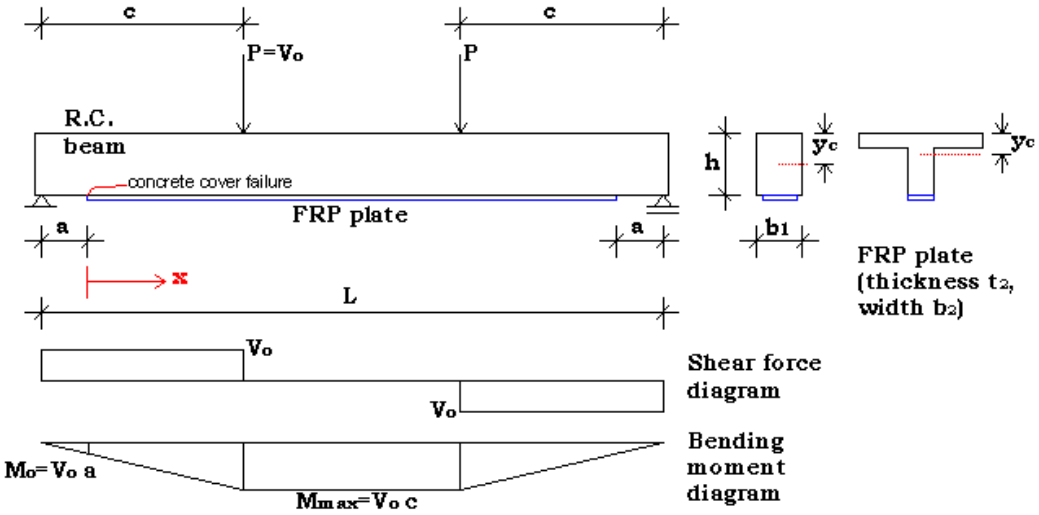

Figure 2: The geometry of FRP-strengthened concrete beam under two point loads.

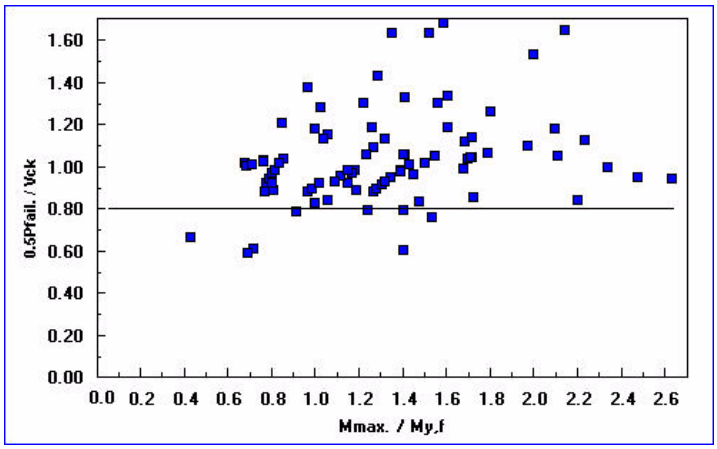

Figure 3: The shear performance of FRP-strengthened beams at failure.

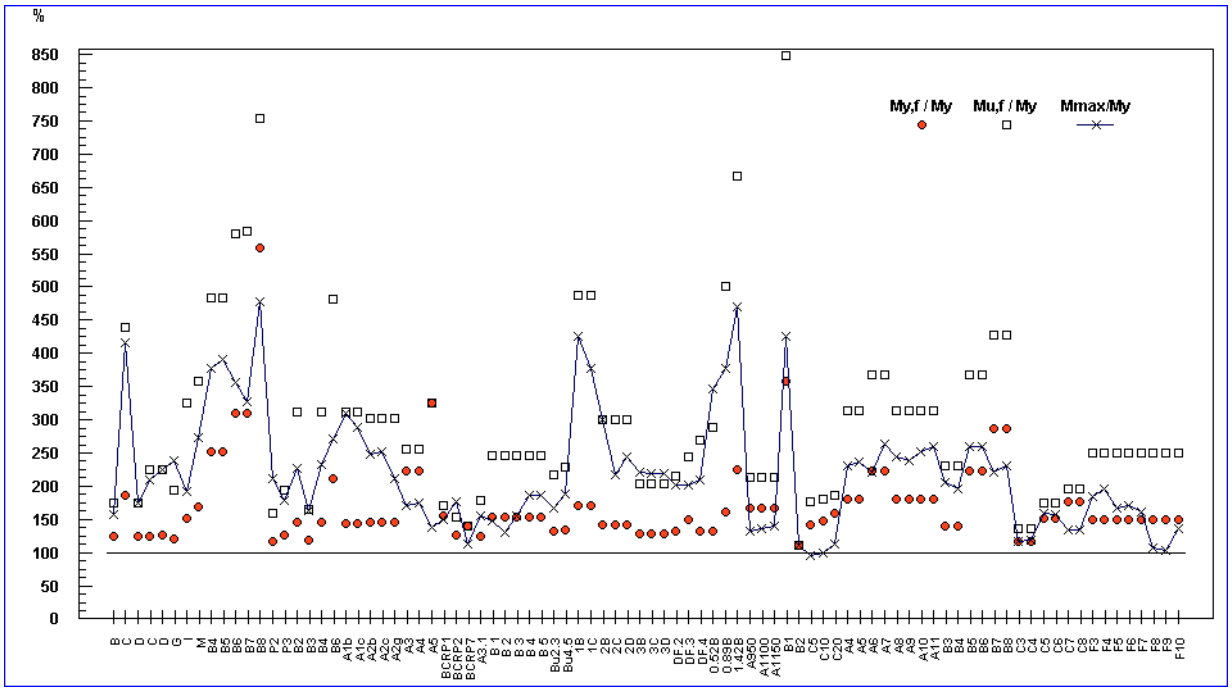

Figure 4: The flexural performance of FRP-strengthened beams at failure.

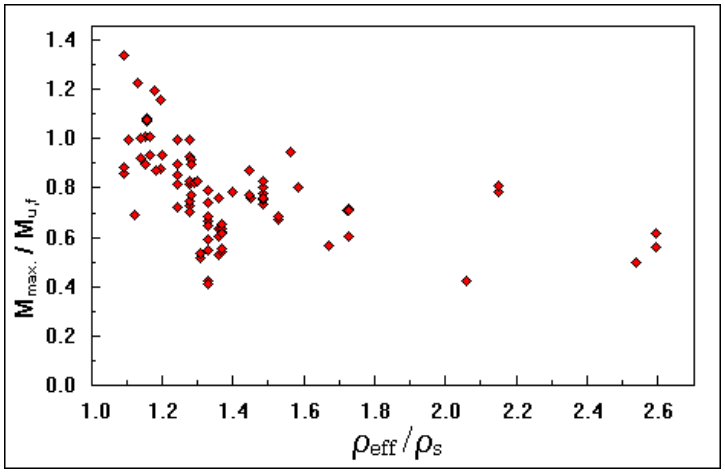

Figure 5: The rate of flexural effectiveness of FRP-strengthened beams (at the point of plate-end debonding) versus FRP-reinforcement ratio.

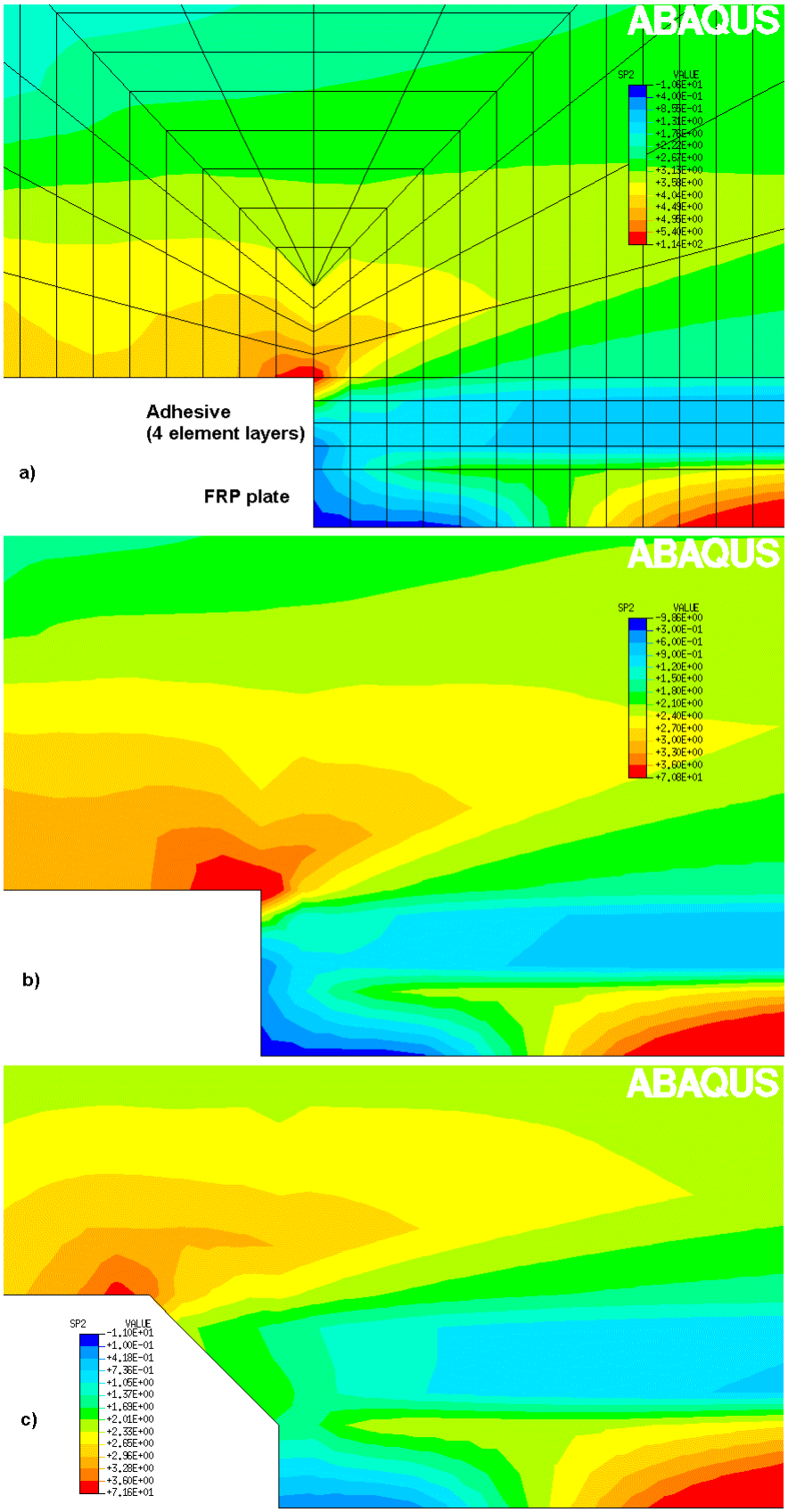

Figure 6: Principal tensile stresses at the end of FRP-plate for beam Bu2.3 [23] a) without reinforcement (max. σ_1=5.41 N/mm²); b) with internal steel reinforcement (max σ_1=3.95 N/mm²) and c) with spew fillet at the adhesive end (max σ_1=3.42 N/mm²).

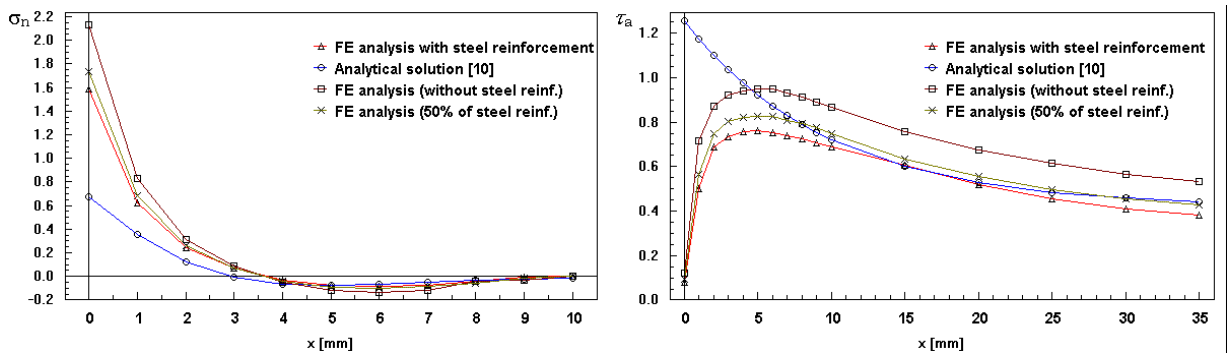

Figure 7: a) Normal peeling and b) shear stresses on the concrete-adhesive interface in the plate anchorage region for beam B6 [20].

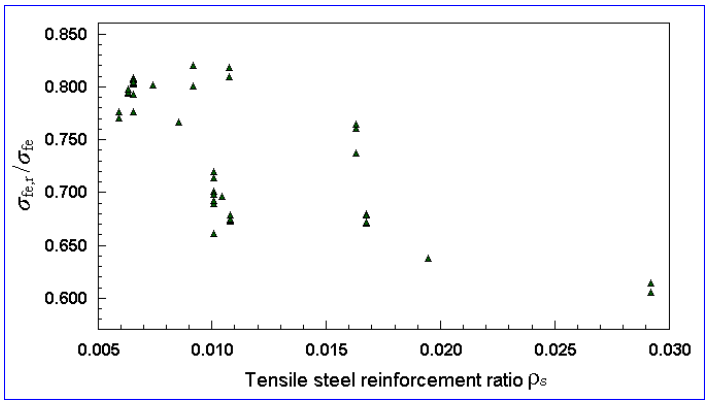

Figure 8: The influence of the tensile steel reinforcement ratio on the reduction of principal tensile stresses in concrete at the plate termination point.

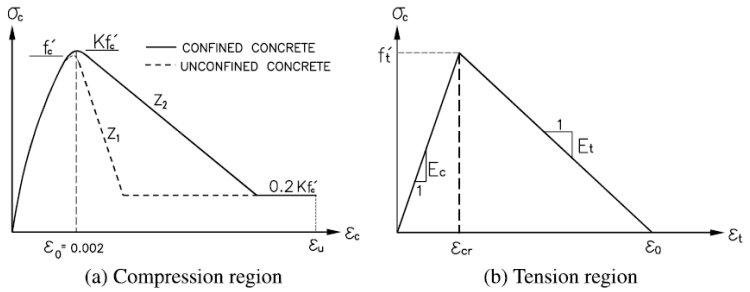

Figure 9: Constitutive model for concrete in compression and tension [34].

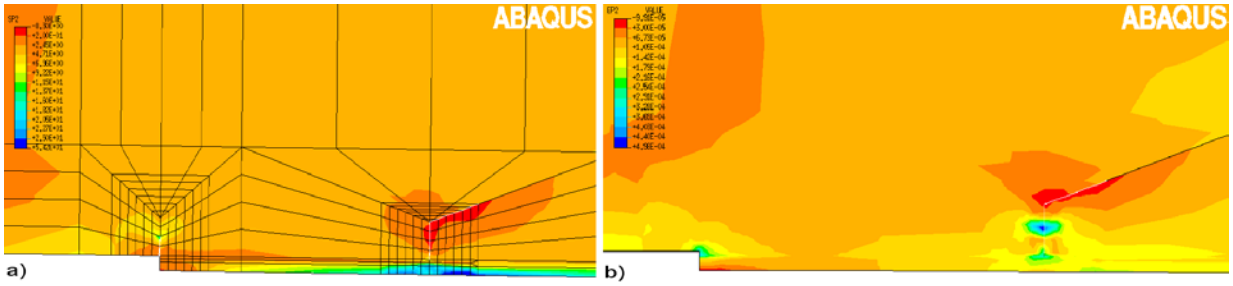

Figure 10: FE model of beam BCRP2 [22]: a) principal tensile stresses at the plate end in the presence of the plate-end and fictive shear cracks; b) principal tensile strains on the concrete-adhesive interface in the presence of shear crack only.

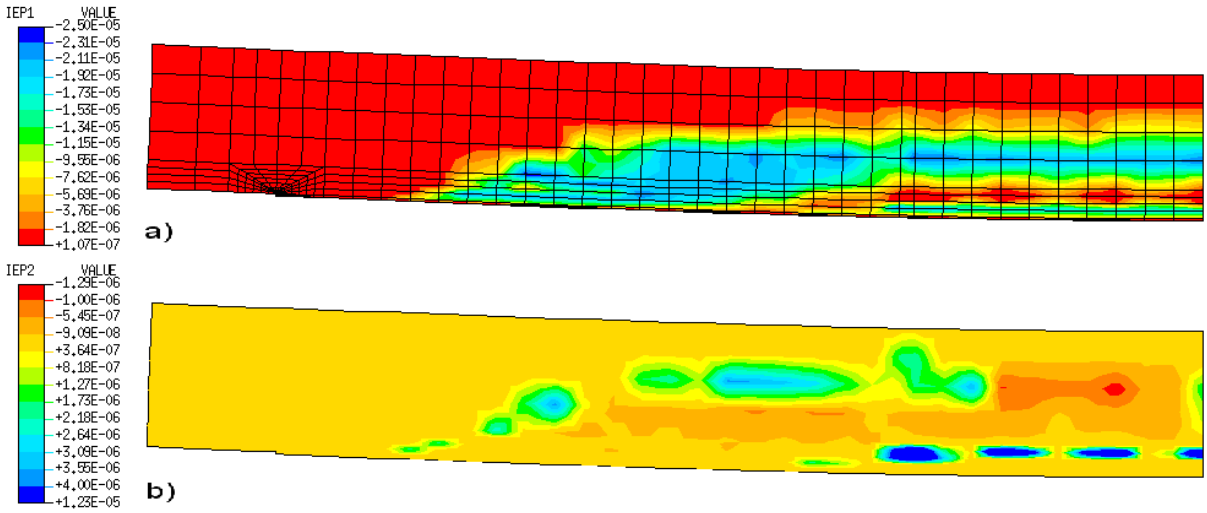

Figure 11: Damage in beam A7 [29] which failed in combined shear and debonding: a) inelastic principal strains IEP1; b) inelastic principal strains IEP2 (one half of the beam modelled due to symmetry and the onset of interface cracking displayed for the 60% of the ultimate failure load).